Phys. Status Solidi RRL **8**, No. 3, 219–222 (2014) / **DOI** 10.1002/pssr.201409040

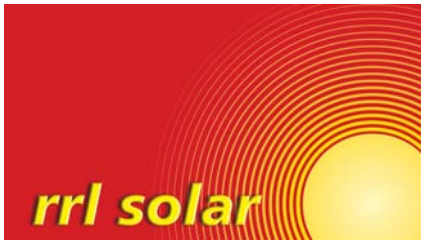

Compositional investigation of potassium doped Cu(In,Ga)Se_2 solar cells with efficiencies up to 20.8%

Philip Jackson*, Dimitrios Hariskos, Roland Wuerz, Wiltraud Wischmann, and Michael Powalla

Zentrum für Sonnenenergie- und Wasserstoff-Forschung Baden-Württemberg (ZSW), Industriestraße 6, 70565 Stuttgart, Germany

Received 22 January 2014, revised 13 February 2014, accepted 13 February 2014
Published online 19 February 2014

Keywords CIGS, thin films, solar cells, composition, efficiency, doping

* Corresponding author: e-mail philip.jackson@zsw-bw.de, Phone: +49 711 7870 260, Fax: +49 711 7870 230

We report on the interaction between intentional potassium doping of thin film Cu(In,Ga)Se_2 (CIGS) solar cells, CIGS absorber composition, and device efficiency. Up to now high efficiency CIGS solar cells could not be produced with a gallium/(gallium + indium) ratio higher than 35%. The new doping process step does not only increase solar cell conversion efficiencies up to 20.8%, but also allows a shift in the CIGS absorber composition towards higher gallium content whilst maintaining this high efficiencies level. We find that the saturation of the open circuit voltages for higher gallium content that is normally observed can partially be overcome by the new doping procedure. This observation leads us to the conclusion that even on this high performance level CIGS solar cells still hold a potential for further development beyond the record values reported here.

1 Introduction For about three years Cu(In,Ga)Se_2 (CIGS) performance-wise has been lingering at the doorstep between the two worlds of thin film and silicon solar technologies [1–3]. The mutually shared threshold value was a solar cell conversion efficiency of 20.4% [4] for both CIGS and multicrystalline silicon. This contribution, however, for the first time can report on an efficiency of 20.8% for a CIGS thin film solar cell that invades this new territory formerly dominated by silicon solar technologies. The key experimental measure that we have taken to accomplish this progress is the intentional post-treatment potassium doping. A positive effect on CIGS solar cell efficiency by the use of potassium as a dopant has first been described in [5] and brought to a significantly advantageous application in [2, 3, 6]. The introduction of this additional doping material, however, has proven to be more than just a minor adjustment in the processing of CIGS, since we have found a major shift of the corridor of viable compositions for high efficiency CIGS solar cells to occur. This paper focuses on these particular changes.

2 Experimental methods

2.1 Processing of CIGS cells The substrate we use for the production of CIGS solar cells is both standard soda-lime glass (3 mm) and for practical purposes also thinner (2 mm) alkali-aluminosilicate glass. The vacuum deposited thin-film stack starts with a layer of sputtered molybdenum (500–900 nm) which delivers the function of the electrical back contact of the solar cells. Then we co-evaporate Cu, In, Ga, and Se to grow the quarternary CIGS semiconductor thin film layer (2.5–3.0 μm) using the 3-stage process. This resulting layer is p-doped by defects in the crystal structure. Further beneficial doping occurs by diffusion of Na from the substrate during the high temperature growth phase. After the CIGS process and during the cool-down phase, we apply a KF post-treatment very similar to the one described in [2, 3]. Correspondingly, we have used substrate temperatures of 350 °C for this procedure and also varying temperatures above that value but with similar results. No further annealing is applied afterwards. Subsequently, the samples are dipped into a chemical bath to form a thin layer of CdS functioning as n-doped buffer layer (30–50 nm). Then back in the vacuum, we sputter undoped ZnO (50–100 nm) and Al-doped ZnO (150–200 nm) as another buffer layer and conductive window material, respectively. Finally, we evaporate a nickel/aluminium grid and the cell size is defined by mechanical scribing. The resulting cell area is

0.50 cm^2 with very little variation. For some of the high-efficiency cells, we also put an anti-reflective coating (ARC) on top of the whole cell stack (MgF_2/105–115 nm). However, in this contribution all solar cell efficiencies are made and measured without the contribution of an ARC except for the record cells referred to in Figs. 1 and 2.

2.2 Characterisation methods For the analysis of the CIGS solar cells current–voltage (*I–V*) analysis was performed under a simulated AM 1.5 G spectrum at 25 °C with a four-point measurement setup. CIGS composition was determined with an X-ray fluorescence spectroscopy (XRF) instrument from EDAX (Eagle XXL). The determined compositional ratio values as the Cu/(Ga + In) (CGI) and Ga/(Ga + In) (GGI) ratios represent average values that do not further specify our compositional grading. How our typical gradings look like can be seen in [7]. The current gradings of CIGS cells with KF do not show any major changes in the general outline of these depth profiles. Thus, the average compositional values are not affected notably by KF post-treatment.

3 Results and discussion The experimental procedure as described above has resulted in a new world record efficiency of 20.8% (with ARC) for thin film solar cells. The area of this solar cell is (0.5005 ± 0.0031) cm^2 determined by an optical method. This area includes the front-contact. The back-contact, however, is outside this cell area as is common for thin film solar cells (when we subtract the front contact and grid area we get an active area efficiency of 21.2%). The *I–V* parameters as depicted in Fig. 1 show a pronounced increase in efficiency η (+0.5%$_{absol.}$) compared to our former record cell (η = 20.3%) [1].

This improvement is due to an increase in open circuit voltage V_{oc} (+17 mV) and fill-factor FF (+1.6%$_{absol.}$) compared to our former record results [1]. However, we have to accept a slight decrease in the short circuit current density J_{sc} (–0.6 mA/cm^2). Compared to the 20.4% cell results on polyimide [2, 3] that have utilised the KF post-

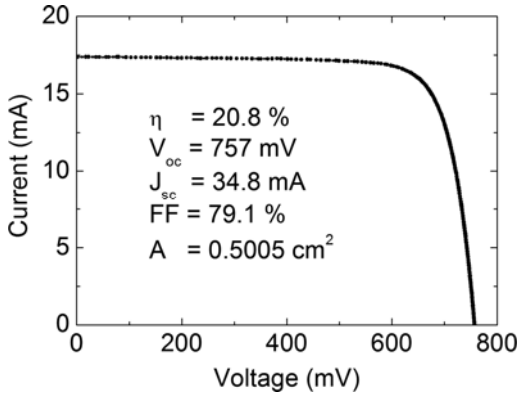

Figure 1 Current–voltage (*I–V*) curve of the new 20.8% (with ARC) record cell as measured and certified by Fraunhofer ISE including cell area.

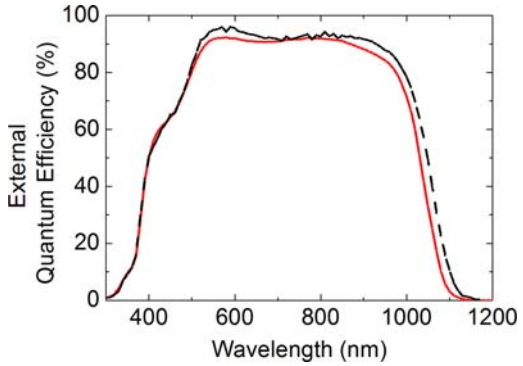

Figure 2 External quantum efficiency (EQE) as measured and certified by Fraunhofer ISE of former (black dashed line) and current record cell (red line) (both with ARC). In the latter a slight loss in the longer wavelength region (800–1000 nm) can be detected.

treatment procedure as well, our results are very similar apart from a clear advantage in V_{oc} (+20 mV). The composition of our 20.8% cell as expressed in the relevant composition ratios (CGI = 0.91 and GGI = 0.32) also deviates from the ranges given in [2] (i.e. CGI: 0.78–0.82 and GGI: 0.33–0.38). So despite the fact that our cell is slightly below the GGI range given in [2], the V_{oc} is significantly higher. Concerning the low J_{sc} values, a comparison of the external quantum efficiency curves (EQE) (Fig. 2) of our current (20.8%) and our former record cell (20.3%) [1] appears to show similar losses due to the KF treatment in the longer wavelength region (800–1000 nm) as also discussed in [3]. The exact loss mechanism in our cells, however, is still open for discussion.

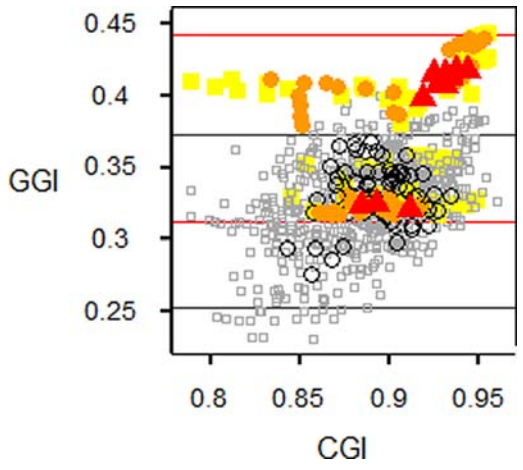

Figure 3 A compositional shift (efficiency vs. GGI vs. CGI) in high efficiency CIGS solar cells occurs when comparing high efficiency CIGS solar cells without KF (grey scale and open symbols) and with KF treatment (yellow to red and closed symbols) towards higher GGI values for the latter group. Efficiency ranges for both groups: □ 18.5% ≤ η < 19.0%; ○ 19.0% ≤ η < 19.5%, and △ 19.5% ≤ η ≤ 20.0% (all *without* ARC).

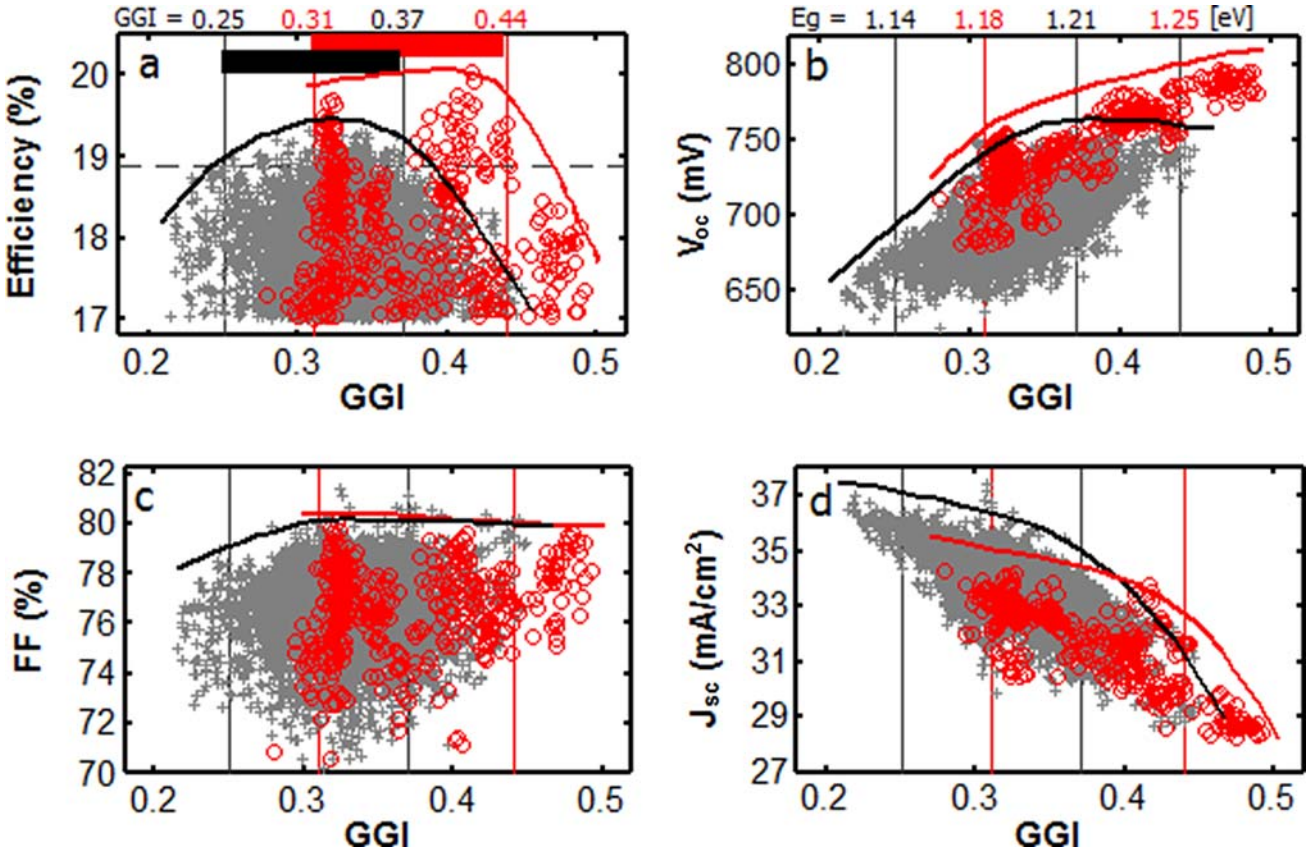

Figure 4 Comparison of cells with $\eta \geq 17.0\%$ (*without* ARC): group A (grey crosses/n(w/o KF) = 6936) represents cells without KF and group B (red open circles/n(KF) = 437) cells with KF post-treatment. The KF treatment enables the extension of the high efficiency corridor in which V_{oc} follows the increase in GGI without saturation.

The new KF procedure, however, seems to generate even more fundamental changes in the CIGS system. One of these is the compositional shift that occurs for high efficiency CIGS solar cells (i.e. $\eta \geq 18.5\%$ w/o ARC; ARC usually adds 1.0%–1.3%$_{absol.}$ in efficiency) when the KF post-treatment is applied. The application of KF does not change the integral composition of the CIGS absorber (determined by XRF) and in general terms it does not change the compositional grading either (compare [6]), but it induces a shift of the compositional corridor for high efficiency cells toward higher GGI ratios. The CGI ratio corridor appears to be more or less unaffected. Figure 3 displays the two relevant experimental groups: group 1, the CIGS cells without KF, is shown in levels of grey (open symbols), and group 2, the CIGS cells with KF, is shown in colours of yellow to red (closed symbols). In each group the square symbols represent the efficiency range $18.5\% \leq \eta < 19.0\%$, the circular symbols $19.0\% \leq \eta < 19.5\%$, and the triangular symbols $19.5\% \leq \eta \leq 20.0\%$ (no data points for group 1 in this last category) (all *without* ARC).

Figure 4 shows a more detailed picture of this correlation between the possible GGI corridor for high efficiencies and the KF post-treatment – this time including all cells with $\eta \geq 17.0\%$ (*without* ARC). Group A (grey crosses/n(w/o KF) = 6936) represents cells without KF and group B (red open circles/n(KF) = 437) cells with KF post-treatment. In the graphs we have included a guide to the eye that loosely resembles an envelope for each dataset. This aid is supposed to facilitate the interpretation. If we first of all look at group A in the efficiency vs. GGI graph in Fig. 4a, we can see that for our experimental setup CIGS solar cells with an efficiency $\eta \geq 18.9\%$ (dashed horizontal line) since recently could only be produced in a corridor of $0.25 \leq \text{GGI} \leq 0.37$ (vertical boundary markers, results in cells with $\eta \geq 20.0\%$ when ARC is applied and when assuming a realistic gain in efficiency of 1.1% by the application of the ARC). Beyond a GGI of 0.37 a clear drop in efficiency occurs for this group A. This trend changes when we look at the new group B. For cells with KF post-treatment this high efficiency corridor shifts to $0.31 \leq \text{GGI} \leq 0.44$ (lower limit is not well established yet due to limited experiments in the low GGI region). In addition, we see an overall increase of the efficiency level in the KF treated group B. The efficiency gain is due to an overall increase in V_{oc} in the range of $0.30 \leq \text{GGI} \leq 0.49$ compared to group A (Fig. 4b). Furthermore, we see a nearly linear proportionality between V_{oc} and GGI for group B over this whole GGI range. This proportional behaviour as such is a well known fact, yet, up to now

standard CIGS solar cells experienced a lamentable saturation in V_{oc} development once the GGI is increased beyond 0.35 [8, 9]. This saturation of V_{oc} for higher Ga content (i.e. higher band gaps E_g) up to now has prevented the progression towards higher band gap CIGS cells. Attempts have been made to break through this barrier [10], but without being able to implement these concepts into CIGS cells with maximum efficiency. The new KF post-treatment (group B), however, seems to partially overcome the V_{oc} saturation in a GGI range of 0.35 to 0.49. Most notably, however, is the fact that maximum efficiencies can be maintained up to a GGI value of approximately 0.44 (i.e. $E_g = 1.25$ eV). At the top of Fig. 4b we have replaced the GGI boundary markers by the corresponding band gap values (using the following formula: $E_g = 1.01(1-x) + 1.65x - 0.15x(1-x)$, with x being the respective GGI value). The FF seems to be unaffected by the KF treatment (Fig. 4c). The J_{sc} values of the KF group B in this higher GGI region appear to be similar to those in group A (Fig. 4d). However, there might be an indication to the fact that for GGI < 0.35 group B looses in J_{sc} relative to group A the more the GGI ratio is reduced (more data points are needed for group B to further undermine this conclusion).

4 Conclusion The new KF post-treatment is more than a minor addition to the traditional CIGS production procedures. It opens up a new pathway to CIGS cells with higher gallium content, higher V_{oc}, and E_g. The compositional shift for high efficiency CIGS solar cells that we have observed shows that only a small addition of potassium to the system allows for the reinvestigation of experimental dependencies of traditional variables in the CIGS production process. This opening up of new experimental avenues and new interactions between experimental variables increases the potential of the CIGS solar technology that has now ventured to enter the realm of silicon solar technology with its new 20.8% record efficiency. Due to the new possibilities for experimentation we expect this new record value to last only for a short time. Efficiencies beyond 21% seem to be very likely to appear rather soon.

Acknowledgements We gratefully acknowledge the support of the ZSW MAT team, in particular that of Dieter Richter for his technical management of the small cell production line and his effort in producing the solar cells. We also thankfully acknowledge the funding by the Bundesministerium für Umwelt, Naturschutz und Reaktorsicherheit (BMU) under contract No. 0329585G.

References

[1] P. Jackson, D. Hariskos, E. Lotter, S. Paetel, R. Wuerz, R. Menner, W. Wischmann, and M. Powalla, Prog. Photovolt.: Res. Appl. **19**, 894 (2011).
[2] A. Chirilă, P. Reinhard, F. Pianezzi, P. Bloesch, A. R. Uhl, C. Fella, L. Kranz, D. Keller, C. Gretener, H. Hagendorfer, D. Jaeger, R. Erni, S. Nishiwaki, S. Buecheler, and A. N. Tiwari, Nature Mater. **12**, 1107 (2013).
[3] F. Pianezzi, P. Reinhard, A. Chirilă, S. Nishiwaki, B. Bissig, S. Buecheler, and A. N. Tiwari, J. Appl. Phys. **114**, 194508 (2013).
[4] M. A. Green, K. Emery, Y. Hishikawa, W. Warta, and E. D. Dunlop, Prog. Photovolt.: Res. Appl. **22**, 1 (2014).
[5] R. Wuerz, A. Eicke, F. Kessler, S. Paetel, S. Efimenko, and C. Schlegel, Sol. Energy Mater. Sol. Cells **100**, 132 (2012).
[6] A. Laemmle, R. Wuerz, and M. Powalla, Phys. Status Solidi RRL **7**, 631 (2013).
[7] M. Powalla, P. Jackson, W. Witte, D. Hariskos, S. Paetel, C. Tschamber, and W. Wischmann, Sol. Energy Mater. Sol. Cells **119**, 51 (2013).
[8] W. N. Shafarman, R. Klenk, and B. E. Mc Candless. 25th IEEE PVSC, Washington DC, USA, 1996, pp. 763–768.
[9] R. Herberholz, V. Nadenau, U. Ruehle, C. Koeble, H. W. Schock, and B. Dimmler, Sol. Energy Mater. Sol. Cells **49**, 227 (1997).
[10] M. A. Contreras, L. M. Mansfield, B. Egaas, J. Li, M. Romero, R. Noufi, E. Rudiger-Voigt, and W. Mannstadt, Prog. Photovolt.: Res. Appl. **20**, 843 (2012).

